EUMETSAT Satellite Application Facility on Climate Monitoring

The EUMETSAT Network of Satellite Application Facilities

CM SAF Climate Monitoring

Algorithm Theoretical Baseline Document

HOAPS version 4.0

DOI: 10.5676/EUM_SAF_CM/HOAPS/V002

Precipitation	CM-12611 (PRE_HOAPS)
Vertically Integrated Water Vapour	CM-12701 (HTW_HOAPS)
Evaporation	CM-12801 (EVA_HOAPS)
Latent Heat Flux	CM-12811 (LHF_HOAPS)
Freshwater Flux	CM-12821 (EMP_HOAPS)
Near Surface Specific Humidity	CM-12901 (NSH_HOAPS)
Near Surface Wind Speed	CM-12911 (SWS_HOAPS)

Reference Number:	SAF/CM/DWD/ATBD/HOAPS/2
Issue/Revision Index:	2.3
Date:	31.01.2017

Document Signature Table

	Name	Function	Signature	Date
Author	Kathrin Graw, Axel Andersson, Marc Schröder, Karsten Fennig	CM-SAF scientists		31.01.2017
Editor	Rainer Hollmann	Science Coordinator		31.01.2017
Approval	Rainer Hollmann	Science Coordinator		31.01.2017
Release	Martin Werscheck	Project Manager		

Distribution List

Internal Distribution	
Name	No. Copies
DWD Archive	1
CM SAF Team	Electronically

External Distribution		
Company	Name	No. Copies
PUBLIC		1

Document Change Record

Issue/ Revision	Date	DCN No.	Changed Pages/Paragraphs
2.0	23/02/2016	SAF/CM/DWD/ATBD/HOAPS/2	First official version.
2.1	06/04/2016	SAF/CM/DWD/ATBD/HOAPS/2	RID answers implemented
2.2	14/11/2016	SAF/CM/DWD/ATBD/HOAPS/2	Update in preparation for DRR2.7
2.3	31.01.2017	SAF/CM/DWD/ATBD/HOAPS/2	RID answers from DRR 2.7 implemented

Applicable and Reference Documents

Doc ID	***Title***	***Reference***
AD 1	FCDR on SSMI/SSMIS Brightness Temperatures, DOI:10.5676/EUM_SAF_CM/FCDR_MWI/V002	SAF/CM/DWD/ATBD/FCDR_SSMIS/1.0
AD 2	UK MetOffice 1D-Var Top-Level Design	NWPSAF-MO-DS-005

RD 1	SAF_CM_DWD_PRD_CDOP2	SAF/CM/DWD/PRD/2.9
RD 2	Algorithm Theoretical Basis Document Fundamental Climate Data Record of SSM/I Brightness Temperatures	SAF/CM/DWD/ATBD/FCDR_SSMI/1.3
RD 3	Diverse profile datasets from the ECMWF 91-level short-range forecasts	NWPSAF-EC-TR-010 v1
RD 4	NWPSAF UK MetOffice 1D-Var User Manual	NWPSAF-MO-UD-032
RD 5	Algorithm Theoretical Basis Document HOAPS version 3.2	SAF/CM/DWD/ATBD/HOAPS/1.1
RD 6	Product User Manual HOAPS version 4.0	SAF/CM/DWD/PUM/HOAPS/2 version 1.1
RD 7	RTTOV v11 Users Guide	NWPSAF-MO-UD-028
RD 8	Validation Report SSM/I products HOAPS release 3.2	SAF/CM/VAL/HOAPS/1.1
RD 9	Data Set Generation Capability Description Document HOAPS release 4.0	SAF/CM/DWD/DGCDD/HOAPS/2.1

Acronyms and Definitions

Table 1 lists definitions for all acronyms used in this document.

Table 1: List of acronyms and definitions.

Symbol	Comment
1D-Var	1 Dimensional Variational
AD	Applicable Document
ATBD	Algorithm Theoretical Baseline Document
AVHRR	Advanced Very-High-Resolution Radiometer
B matrix	Background error covariance matrix
BMBF	German Federal Ministry of Education and Research
CDRs	Climate Data Records
CDOP2	Continuous Development and Operations Phase
CM SAF	Satellite Application Facility on Climate Monitoring
COARE	Coupled Ocean-Atmosphere Response Experiment
DFG	Deutsche Forschungsgemeinschaft
DMSP	Defence Meteorological Satellite Program
DWD	Deutscher Wetterdienst
ECMWF	European Centre for Medium-Range Weather Forecasts
ECVs	Essential Climate Variables
EIA	Earth Incidence Angle
EUMETSAT	European Organization for the Exploitation of Meteorological Satellites
EVA	Evaporation
FCDRs	Fundamental Climate Data Records
EMP	Freshwater Flux
F08	DMSP Flight-08 spacecraft, F10-F20 accordingly
FMI	Finnish Meteorological Institute
GCOS	Global Climate Observing System

Symbol	Comment
GHRSST	Group for High Resolution Sea Surface Temperature
h	horizontal
HOAPS	Hamburg Ocean Atmosphere Parameters and Fluxes from Satellite Data
HTW	Vertically Integrated Water Vapour
ICOADS	International Comprehensive Ocean-Atmosphere Data Set
KNMI	Royal Meteorological Institute of the Netherlands
L3	Level 3 data (gridded data of geophysical parameters)
LHF	Latent Heat Flux
LWP	Liquid Water Path
MeteoSwiss	Meteorological Service of Switzerland
MiKlip	Mittelfristige Klimaprognosen (project funded by BMBF)
NetCDF	Network Common Data Format
NMHSs	National Meteorological and Hydrological Services
NOAA	National Oceanic and Atmospheric Administration
NSH	Near Surface Specific Humidity
NWP SAF	Satellite Application Facility on Numerical Weather Prediction
OE	Optimal Estimation
OISST	Optimum Interpolation Sea Surface Temperature
q	Specific humidity
PRD	Product Requirements Document
PRE	Precipitation
RAM	Random Access Memory
RD	Reference Document
$\boldsymbol{R}$ matrix	Observational error covariance matrix
RMIB	Royal Meteorological Institute of Belgium
RTTOV	Radiative Transfer for TOVS

Symbol	Comment
SMHI	Swedish Meteorological and Hydrological Institute
SSM/I	Special Sensor Microwave/Imager
SSM/T	Special Sensor Microwave Temperature
SSM/T-2	Special Sensor Microwave Humidity Sounder
SSMIS	Special Sensor Microwave Imager/Sounder
SSMI(S)	SSM/I and SSMIS
SST	Sea Surface Temperature
SWS	Near Surface Wind Speed
Tb	Brightness Temperature
TIROS	Television and InfraRed Observation Satellite
TOVS	TIROS Operational Vertical Sounder
Tskin	Skin Temperature
Tsurf	Surface Temperature
UK MetOffice	Meteorological Service of the United Kingdom
v	vertical
WCRP	World Climate Research Program
WMO	World Meteorological Organization

Table of Contents

List of Figures

List of Tables

1 The EUMETSAT SAF on Climate Monitoring

The importance of climate monitoring with satellites was recognized in 2000 by EUMETSAT Member States when they amended the EUMETSAT Convention to affirm that the EUMETSAT mandate is also to "contribute to the operational monitoring of the climate and the detection of global climatic changes". Following this, EUMETSAT established within its Satellite Application Facility (SAF) network a dedicated centre, the SAF on Climate Monitoring (CM SAF, http://www.cmsaf.eu/).

The consortium of CM SAF currently comprises the Deutscher Wetterdienst (DWD) as host institute, with partners from the Royal Meteorological Institute of Belgium (RMIB), the Finnish Meteorological Institute (FMI), the Royal Meteorological Institute of the Netherlands (KNMI), the Swedish Meteorological and Hydrological Institute (SMHI), the Meteorological Service of Switzerland (MeteoSwiss), and the Meteorological Service of the United Kingdom (UK MetOffice). Since the beginning in 1999, the EUMETSAT Satellite Application Facility on Climate Monitoring (CM SAF) has developed and will continue to develop capabilities for a sustained generation and provision of Climate Data Records (CDR's) derived from operational meteorological satellites.

In particular the generation of long-term data records is pursued. The ultimate aim is to make the resulting data records suitable for the analysis of climate variability and potentially the detection of climate trends. CM SAF works in close collaboration with the EUMETSAT Central Facility and liaises with other satellite operators to advance the availability, quality and usability of Fundamental Climate Data Records (FCDRs) as defined by the Global Climate Observing System (GCOS). As a major task the CM SAF utilizes FCDRs to produce records of Essential Climate Variables (ECVs) as defined by GCOS. Thematically, the focus of CM SAF is on ECVs associated with the global energy and water cycle.

The CM SAF data records can serve applications related to the new Global Framework of Climate Services initiated by the WMO World Climate Conference-3 in 2009. CM SAF is supporting climate services at national meteorological and hydrological services (NMHSs) with long-term data records but also with data records produced close to real time that can be used to prepare monthly/annual updates of the state of the climate. Both types of products together allow for a consistent description of mean values, anomalies, variability, and potential trends for the chosen ECVs. CM SAF ECV data records also serve the improvement of climate models both at global and regional scale.

A catalogue of all available CM SAF products is accessible via the CM SAF webpage, http://www.cmsaf.eu/. Here, detailed information about product ordering, add-on tools, sample programs and documentation is provided.

1 Introduction

This Algorithm Theoretical Baseline Document (ATBD) provides information on the processing chain implemented for the enhanced HOAPS (Hamburg Ocean Atmosphere Parameters and Fluxes from Satellite Data, http://www.hoaps.org/) thematic climate data record. This processing chain retrieves geophysical parameters from homogenized SSM/I (Special Sensor Microwave/Imager) and SSMIS (Special Sensor Microwave Imager/Sounder) observations. Auxiliary information from AVHRR (Advanced Very-High-Resolution Radiometer) SST (Sea Surface Temperature) retrievals and a predefined database of atmospheric background profiles is required for the retrieval. Compared to the previous HOAPS version 3.2 (cf. Andersson et al., 2010 and RD 5) a one-dimensional variational retrieval (1D-Var) scheme is used to derive a subset of the geophysical parameters. The 1D-Var retrieval is based on that of the UK MetOffice NWP SAF (Satellite Application Facility on Numerical Weather Prediction). Preliminary work for the HOAPS 1D-Var retrieval for precipitation has been done within the MiKlip Project (mittelfristige Klimaprognose, German Federal Ministry of Education and Research (BMBF)).
The HOAPS data record contains multiple parameters derived from SSM/I and SSMIS observations. The CM SAF version of HOAPS-4.0 contains the following atmospheric and near-surface variables, derived for the global ice-free oceans:

Precipitation	CM-12611 (PRE_HOAPS)
Vertically Integrated Water Vapour	CM-12701 (HTW_HOAPS)
Evaporation	CM-12801 (EVA_HOAPS)
Latent Heat Flux	CM-12811 (LHF_HOAPS)
Freshwater Flux	CM-12821 (EMP_HOAPS)
Near Surface Specific Humidity	CM-12901 (NSH_HOAPS)
Near Surface Wind Speed	CM-12911 (SWS_HOAPS)

The 1D-Var retrieves vertically integrated water vapour and near surface wind speed. The retrieval procedure of the remaining parameters has not been changed from HOAPS-3.2. Precipitation is derived using a neural network algorithm. The parameterization of the latent heat flux has not been changed either, but uses the results from the 1D-Var retrieval as input. The physical basis of the HOAPS-3.2 retrievals is described in RD 5 and in this document a summary is given in section 3.3.
Within the project FOR1740 of the Deutsche Forschungsgemeinschaft (DFG) a procedure to estimate uncertainty for evaporation and related parameters has been developed. This approach has been adapted to the new HOAPS-4.0 data record and the resulting uncertainty estimates are also provided with HOAPS-4.0.
This ATBD focuses on information on the HOAPS 1D-Var retrieval scheme used to construct the data record employing observations of SSM/I passive microwave radiometers on board Defence Meteorological Satellite Program (DMSP) platforms F08, F10, F11, F13, F14 and F15 as well as observations of SSMIS instruments on board F16, F17 and F18.
The CM SAF HOAPS data record from SSMI(S) (this abbreviated form is used from now on for SSM/I and SSMIS) provides quasi-global coverage over the ice-free ocean surface, i.e., within ±180° longitude and ±80° latitude. Instantaneous SSMI(S) retrievals at original swath level are used to derive the spatio-temporal averaged data records. The products are available as both 6-hourly composites and monthly averages on a regular latitude/longitude grid with a spatial resolution of 0.5° × 0.5° degrees. The temporal coverage of the data records ranges from 9th July 1987 to 31st December 2014 as required by the PRD. Future updates including an extension of the time period are foreseen for CM SAF's next phase. More detailed information on the products and data format specifications of HOAPS-4.0 are given in the Product User Manual HOAPS version 4.0 [RD-6].

Section 2 of this document describes the data sources and processing chain, including a summary of instrument characteristics. This is followed by the Algorithm Theoretical Basis of the 1D-Var scheme as well as assumptions and limitations.
More information on the data record will be contained in the product user manual, basic accuracy requirements are defined in the product requirements document [RD-1], and the validation of the data records versus those requirements is described in the validation report.

2 Input data, pre-processing and algorithm overview

An overview of the full (1D-Var and statistical) retrieval is provided in section 2.5. The 1D-Var code is capable of processing data from various instruments (here: SSM/I and SSMIS, see sections 2.1 and 2.2) using RTTOV as the forward model to obtain simulated radiances and Jacobians with respect to atmospheric state parameters that affect the radiances (Hocking et al., 2014, [RD-7]). Also, the 1D-Var requires a-priori information on the atmospheric state as input. For HOAPS-4.0 an objective profile selection scheme has been developed to construct a background profile from a profile data base (Chevallier et al. 2006, [RD-3], see section 3.2). For some parameters statistical retrievals are applied which are described in section 3.3, see also [RD-5]. SST data (Reynolds et al. 2007, Reynolds 2009, see section 2.3) is required as additional input for some of these parameters.

2.1 Observing Systems: SSMI(S) Instruments

This section gives a short overview of the observing systems (cf. [AD 1]) used to collect the basis input data for the processing of HOAPS-4.0. SSM/I sensors have been carried aboard the DMSP satellite series since 1987. To date, six SSM/I instruments have been successfully launched aboard the F08, F10, F11, F13, F14 and F15 spacecraft. A short summary of the SSM/I instrument is given in RD-5 and references therein. The first SSMIS was launched in October 2003 aboard the F16 spacecraft, designed to continue the successful SSM/I observations. To date, four SSMIS instruments have been launched (F16, F17, F18, F19) and one more (F20) will be launched in 2020 (Figure 1 and Figure 2). However, data of F19 have not been used for processing HOAPS-4.0. A power failure affecting the command-and-control system on board the F19 spacecraft caused that since 2016 NOAA operators are unable to control F19 which was launched in 2014. The quality of the data of F19 is expected to be degraded (Gruss, 2016).

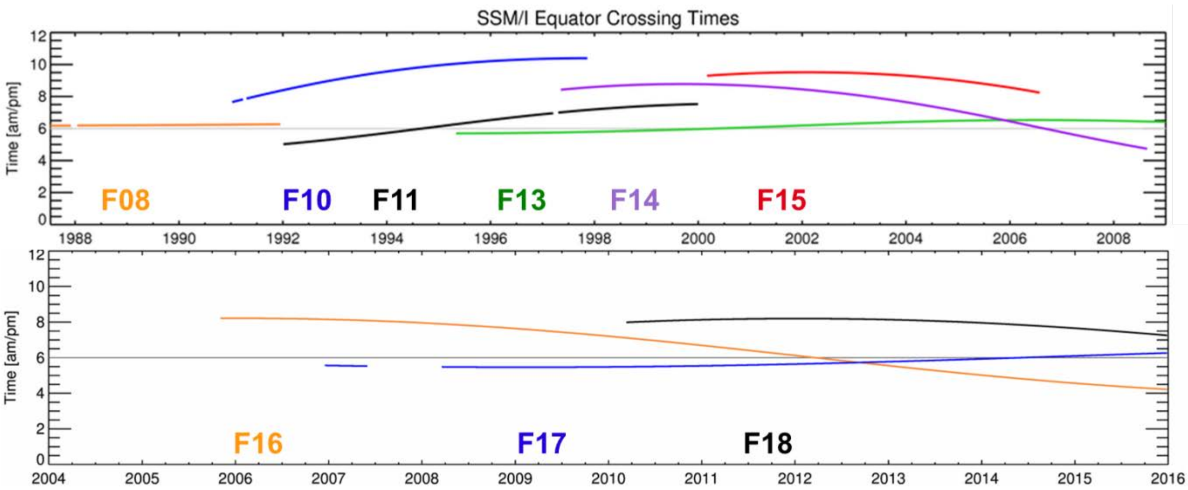

Figure 1: Temporal coverage of SSM/I (top panel) and SSMIS (bottom panel) aboard DMSP satellite platforms used for HOAPS-4.0 processing. Due to orbit degradation the descending equatorial crossing times for all instruments change over time. Some satellite orbits are more stable than others and for some little change occurs over the years of operation.

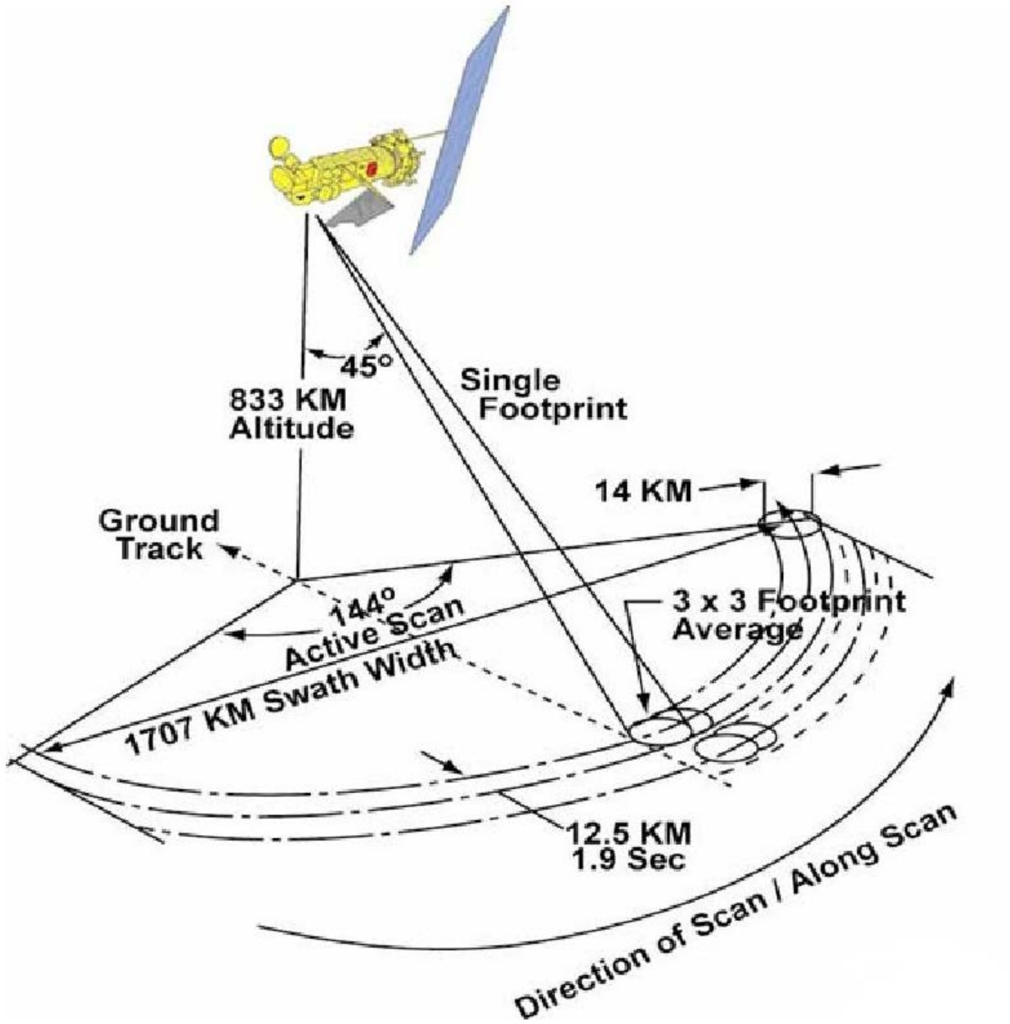

Figure 2: SSMIS scan geometry showing directions of active scan, swath width, ground track, and footprint averages (from Kunkee et al., 2008).

An extensive description of the SSMIS instrument and satellite characteristics has been published by Kunkee et al. (2008). Hence, only a short summary is given here. The DMSP satellites operate in a near-circular, sun-synchronous orbit, with an inclination of 98.8° at an approximate altitude of 833 km. Each day, 14.1 orbits with a period of about 102 minutes are performed. The Earth's surface is sampled with a conical scan at a constant antenna boresight angle of 45° over an angular sector of 144° resulting in a 1700 km wide swath (see Figure 2). The advantage of a conical scanning instrument is that it never observes the surface of the earth from nadir, but from a constant angle, thus the path through the atmosphere has always the same length and consequently the same characteristics of the atmosphere. A nearly complete coverage of the Earth by one instrument is achieved within two to three days. Due to the orbit inclination and swath width, the regions poleward of 87.5° are not covered. Note that the final product coverage is within ±80° latitude, because the HOAPS products are only defined over ice free ocean. All satellites have a local equator crossing time between 2 and 11 A.M./P.M. for the descending/ascending node.
The SSMIS integrates the imaging capabilities of the SSM/I sensor with the cross-track microwave sounders Special Sensor Microwave Temperature SSM/T and Special Sensor Microwave Humidity Sounder, SSM/T-2 into a single conically scanning 24-channel instrument. The SSMI(S) frequencies are centred at 19.35, 22.235, and 37.0 GHz. Another frequency is centred at 85.5 GHz for SSM/I and at 91.35 GHz for SSMIS because the

channel 85.5 GHz is not included on SSMIS. All frequencies are sampled at both horizontal and vertical polarizations, except for the 22.235 GHz channel, which measures only vertically polarized radiation. The channels will be referred to as 19, 22, 37, and 91 GHz hereafter.

The spatial resolution varies from 74 km by 47 km for the 19 GHz channel to 15 km by 13 km for the 91 GHz channel. All channels are sampled, resulting in an along-track sampling of 12.5 km with a resolution of 180 uniformly spaced pixels, while the channels 19, 22 and 37 are sampled with a resolution of 90 (64) pixels for SSMIS (SSM/I), i.e., 25 km (see Figure 2). A fixed cold space reflector and a reference black body hot load are used for continuous on-board two point calibration (see section 4.3 in [AD-1]).

2.2 The CM SAF SSM/I and SSMIS FCDR

The SSM/I and SSMIS FCDR (Fennig et al. 2015, AD 1) provides swath-based brightness temperatures (Tbs) for the global ice-free ocean as a basis for the processing of HOAPS-4.0. The CM SAF FCDR from SSMI(S) Tbs is compiled as daily collections of all observations from each sensor. All sensor specific data available in the raw data records are provided as well as additional information like quality control flags, Earth incidence angles (EIA), averaged 85 GHz brightness temperatures, incidence angle normalisation offsets, intersensor calibration offsets and uncertainty information as well as surface type including sea ice. The FCDR is available for the time period from July 1987 until end of 2013.
A more detailed description of the algorithm used to generate the SSMI(S) FCDR can be found in [AD 1].
The extended CM SAF SSMI(S) FCDR which consists of the SSM/I and SSMIS FCDR (Fennig et al., 2015) and a temporal extension of the SSMIS FCDR to 2014 using unchanged algorithms will be used here.

2.3 OISST

The NOAA 0.25° daily Optimum Interpolation Sea Surface Temperature (OISST) (Reynolds et al., 2007; Reynolds, 2009) has been used as input for the processing of HOAPS-4.0 as it is available for the entire time period 1987 – 2014 covered by HOAPS-4.0. The AVHRR Pathfinder sea surface temperature (SST) used for HOAPS-3.2 is unavailable past 2012 and the ESA CCI SST covers the years 1991 – 2010 only. Therefore, the OISST was selected to maintain consistency of the SST for the entire HOAPS record.
The daily OISST is an analysis constructed at the NOAA National Climatic Data Center. For HOAPS-4.0 the daily OISST data files (version 2, AVHRR only) distributed through the Group for High-Resolution Sea Surface Temperature (GHRSST) are used (ftp://ftp.nodc.noaa.gov/pub/data.nodc/ghrsst/L4/GLOB/NCEI/AVHRR_OI/).
Daily gridded OISST fields are constructed by combining observations from satellites and in situ data from ships and moored and drifting buoys obtained from the International Comprehensive Ocean–Atmosphere Data Set (ICOADS version 2.5, Woodruff et al. 2011).
The in situ SSTs are checked for outliers, and then averaged onto the 0.25° grid, separately for ships and buoys. The broad-scale offset between SST observations from ships and those from buoys is accounted for by subtracting a constant value of 0.14°C from the ship observations. Similarly, satellite temperatures are averaged onto the analysis grid, after which they are bias-adjusted to the in situ data. For the marginal ice zone, where there is little in situ data, proxy SSTs are generated from sea ice concentrations. The interpolation step (“Optimum Interpolation”) combines the prepared inputs. The data record also includes sea ice concentrations. However, these are not used for the subsequent processing as the CM SAF FCDR includes its own sea ice mask.

Latent and sensible heat fluxes are estimated with a COARE bulk aerodynamic approach (COARE 3.0) after Fairall et al. (1996, 2003), see Andersson et al. (2010). As in the previous version, this algorithm will be used in HOAPS-4.0 using a skin SST as one of the input parameters. As the OISST is not a skin SST but a bulk SST at 0.5 m, the processing includes the Donlon et al. (2002) approach to calculate the skin temperature utilizing the HOAPS wind speed estimates.
This adjustment does not consider heating of the upper ocean layers during day time. Note that systematic and random uncertainties are computed in a post-processing step following Kinzel et al. (2016), see also section 3.4. These uncertainties are a function of the utilised SST reference.

2.4 Pre-processing

Pre-processing involves the aggregation of the daily OISST-files to yearly files.

2.5 Overview of processing chain

The processing chain implemented for the HOAPS-4.0 data record to retrieve geophysical parameters from the CM SAF SSMI(S) FCDR and auxiliary information from OISST is schematically illustrated in Figure 3. The HOAPS software processor is a collection of tools to produce L2 (swath-based) and L3 (gridded) products. In Figure 3 the processing chain to perform the 1D-Var retrieval is presented. The 1D-Var retrieves total column water vapour and near surface wind speed. The remaining parameters are retrieved with statistical retrievals (section 3.3) as for HOAPS-3.2 (c.f. RD-5). Note that the parameterization of the latent heat flux has not been changed either, but uses the results from the 1D-Var retrieval as input.
The starting point in the data processing chain, as illustrated in Figure 3 are SSMI(S) brightness temperatures. With the additional input of background profiles and OISST, geophysical parameters are calculated on the native sensor resolution (HOAPS-S). Gridded HOAPS products are generated from the scan-based HOAPS-S data with additional gridding routines.

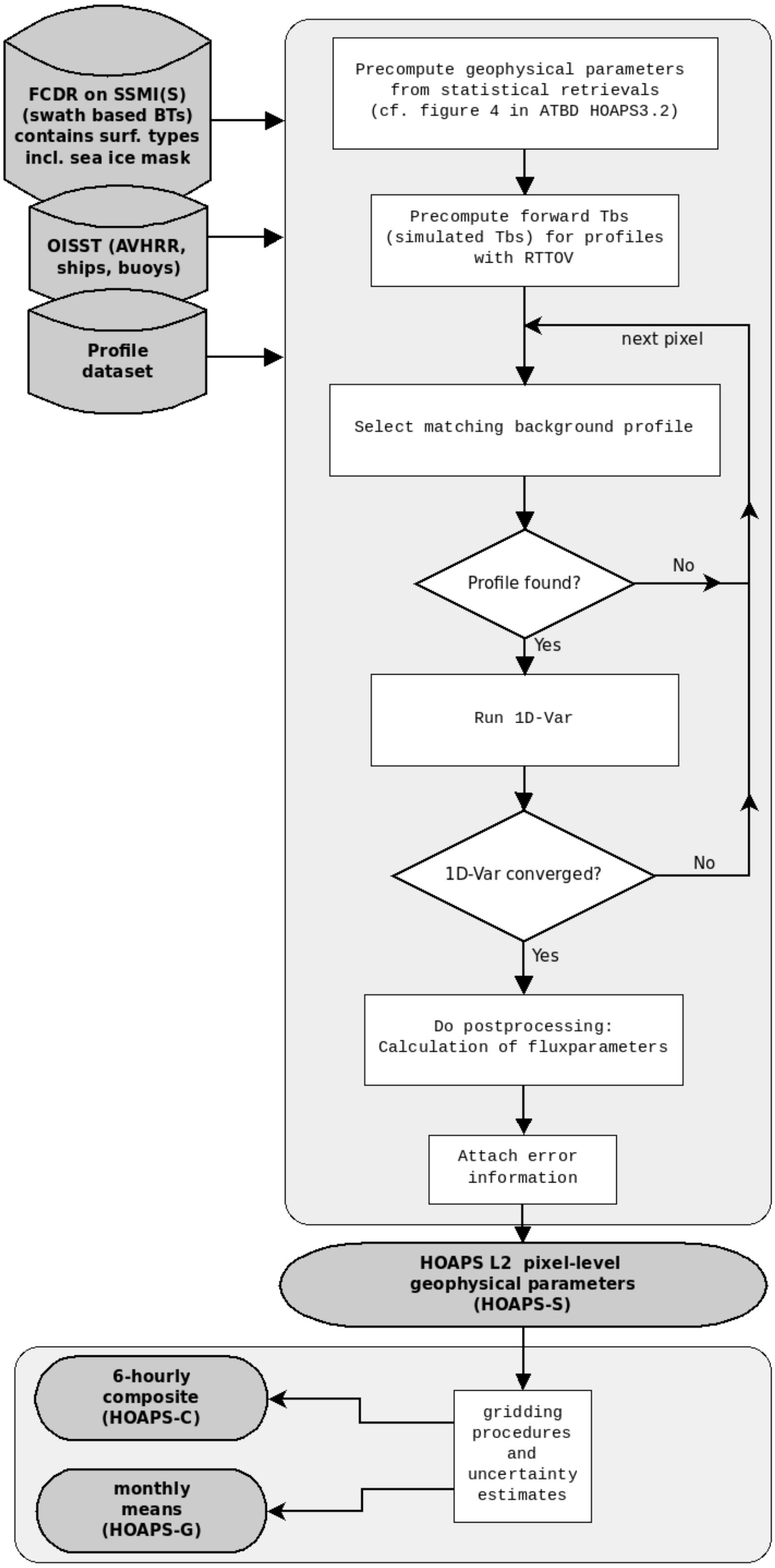

Figure 3: Flow chart for the processing chain in HOAPS-4.0. RTTOV is the radiative-transfer model used in the HOAPS processing.

3 Algorithm Theoretical Basis

The main improvement in HOAPS-4.0, relative to HOAPS-3.2, is the implementation and improvement of the 1D-Var retrieval developed by the NWP SAF and the estimation of uncertainty for evaporation and related parameters. The 1D-Var is applied to retrieve vertically integrated water vapour and near surface wind speed. This retrieval was adapted to the processing of SSMI(S) data by CM SAF utilizing the microwave imager channels and is the focus of this section. The remaining parameters are derived with the HOAPS-3.2 retrievals [RD-5]. The retrievals are implemented on the SSM/I pixel level data. Due to the improved sampling and the larger swath width of SSMIS compared to SSM/I only every second scanline of SSMIS is processed and not all pixels of SSMIS (only 64 from 90) are used to conform with the SSM/I data.

The NWP SAF 1D-Var is a variational method used for the retrieval of the HOAPS-4.0 parameters TCWV and near surface wind speed. Phalippou (1996) presented a similar 1D-Var retrieval and a stand-alone SSM/I, SSMIS and AMSU 1D-Var scheme that was available from NWP SAF. The code of the NWP SAF 1D-Var contains the merged capabilities of the previously supported UK MetOffice and ECMWF 1D-Var schemes, i.e., the NWP SAF partners ECMWF and the Met Office have developed, in parallel, different 1D-Var codes. The HOAPS 1D-Var retrieval is an implementation of the NWP SAF MetOffice package with adaptions for the HOAPS processing chain.
In a variational retrieval the a-priori or background information of the atmosphere and surface, and the measurements (observed Tbs) are combined in a statistically optimal way to estimate the most probable atmospheric state.
The method is based on nonlinear optimal estimation theory, and its context in satellite data assimilation has been discussed by Rodgers (1976) and Eyre (1989). The algorithm is applicable for both daylight and night-time scenes as backscattered microwave radiation is used as input. However, the highly uncertain emissivity of land surfaces and ice or snow covered scenes at microwave frequencies restricts the application of the retrieval to open ocean pixels. A further limitation is the perturbation of microwave signals by heavy precipitation events. Under these conditions the atmosphere is opaque for the retrieval of surface parameters. Additionally, the retrieval is not able to handle scattering effects of hydrometeors properly in such situations and will either not converge or introduce large uncertainties in the retrieved quantities.

The 1D-Var retrieval requires a background profile as input to derive a first guess of atmospheric state. This background profile may stem from a NWP or reanalysis model or concerning the HOAPS climatology it is selected from a predefined data base (see section 3.2).
The geophysical variables from the first guess are mapped into radiance space with the help of a radiative-transfer model (RTTOV), i.e. RTTOV calculates Tbs for channel-specific wavelengths based on atmospheric background fields. RTTOV also includes a fast emissivity model of the ocean surface, FASTEM (Deblonde, 2001; Deblonde et al., 2007). The variational approach applied here enables the simultaneous deduction of different parameters and is therefore an efficient way of extracting information from satellite radiances by using a-priori information (Phalippou, 1996). A minimization procedure searches the optimal solution, which, if successful, is written to output retrieval files accompanied with further diagnostic data.

3.1 Physical Basis Overview of 1D-Var retrieval

The following terminology is used (for details see Rodgers, 2000):

- The state vector ($\boldsymbol{x}$) consists of the quantities retrieved by the optimal estimation (OE) retrieval.
- The observation vector ($\boldsymbol{y}$) holds observed brightness temperatures.
- The a-priori ($\boldsymbol{x}^b$) is the solution to which the state vector will converge in the absence of measurements.

The terminology is adapted from Bayesian estimation and 'a-priori' refers to the a-priori knowledge about the state. In data assimilation a-priori is often used synonymously with 'background'. $\boldsymbol{x}^b$ is therefore the best estimate of the state $\boldsymbol{x}$ in the absence of additional constraining observations ($\boldsymbol{y}$).The a-priori can be determined e.g. from an NWP model, from climatological estimates or from a data base of the state vector $\boldsymbol{x}$. Here a profile is used that has been constructed from a predefined profile data base (see section 3.2) The lower temperature layers of the selected background profile are adjusted to match the actual sea surface temperature.

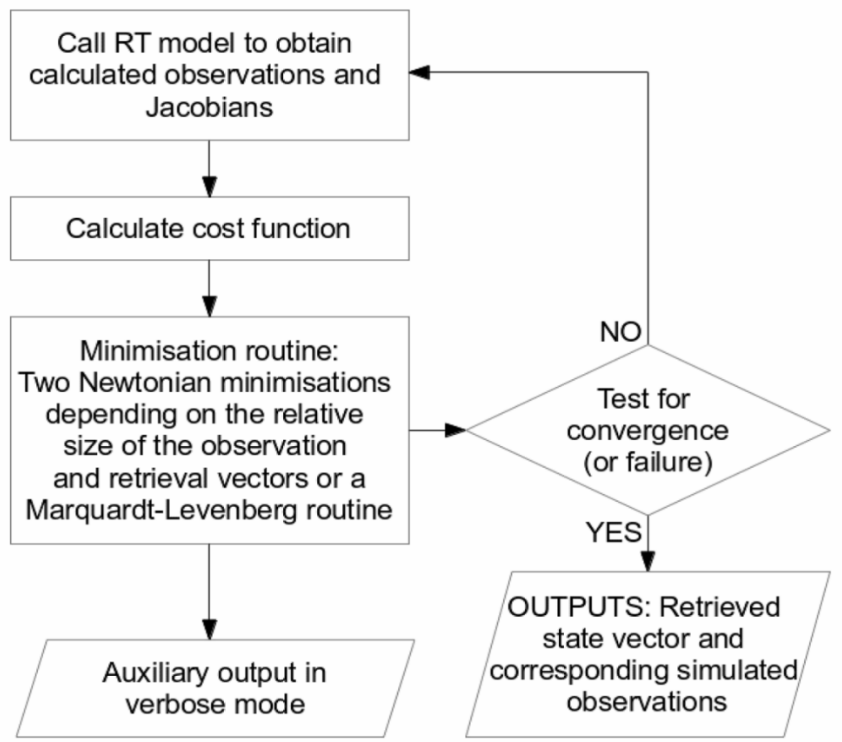

Figure 4: Flowchart of the 1D-Var minimization and output procedures [AD 2]. For HOAPS-4.0 the Marquardt-Levenberg routine is used for minimisation.

The remaining quantities required to set up the equation of the cost function which has to be minimised during the 1D-Var are:

- Background error covariance ($\boldsymbol{B}$): The uncertainty of the a-priori information is characterized by the background error covariance matrix.
- First guess ($\boldsymbol{x}_o$): The first guess consists of the initial values of the state vector when the OE process is started. The first guess can be identical to the a-priori but can also be chosen differently, for example by a first retrieval estimate of the state vector, e.g., from statistical retrievals. The first guess for HOAPS-4.0 is the same as the background.
- Observation operator ($H(\boldsymbol{x})$): maps from state space into observation space. Here, a radiative transfer model (RTTOV) is applied (see below).

- Observation error covariance matrix ($\boldsymbol{R}$): describes uncertainties associated with observation vector $\boldsymbol{y}$. These include sensor noise but also e.g. uncertainties caused by parameterizations in the radiative transfer model.

The 1D-Var scheme searches for the best estimate of atmospheric and/or surface variables (called state vector or control vector) by weighting the a-priori or background vector and the coincident satellite observation vector according to their uncertainties. Integrated over the spectral response function of the selected channels, RTTOV calculates the Tb corresponding to the first-guess atmospheric state.
An optimal state is found for which the expected analysis variance is minimal (Deblonde et al., 2007). This is achieved as follows (see also Figure 4): 1D-Var maximizes the probability density function by minimizing the cost function

$$\boldsymbol{J}(\boldsymbol{x}) = \frac{1}{2}\left(\boldsymbol{x}-\boldsymbol{x^b}\right)^{\boldsymbol{T}}\boldsymbol{B}^{-1}\left(\boldsymbol{x}-\boldsymbol{x^b}\right)+\frac{1}{2}\left[\boldsymbol{H}(\boldsymbol{x})-\boldsymbol{y^0}\right]^{\boldsymbol{T}}\boldsymbol{R}^{-1}\left[\boldsymbol{H}(\boldsymbol{x})-\boldsymbol{y^0}\right] \qquad 3\text{-}1$$

where $\boldsymbol{x}$ is the control vector, $\boldsymbol{x}^b$ is the a-priori or model derived background, $\boldsymbol{y}^o$ are the observations (SSMI(S) brightness temperatures), and $\boldsymbol{B}$ is the background error covariance matrix.
The state vector or control vector $\boldsymbol{x}$ may contain the following variables:

Profiles:

- Humidity*,
- Temperature.

Scalars:

- Surface temperature,
- Cloud liquid water (total column),
- Skin Temperature,
- Surface u wind*,
- Surface v wind*,
- Surface Humidity,
- Surface liquid precipitation flux (rain),
- Surface solid precipitation flux (snow),
- Ice water path.

where the variables labelled with an asterisk are used within generating HOAPS-4.0. The cost function is minimized across all parameters of the control vector simultaneously. The observation error matrix $\boldsymbol{R}$ is mainly composed of the instrumental error and the error of the RTTOV model. RTTOV acts as an observation operator, which computes Tb from first-guess input.
In order to minimize the cost function $J(\boldsymbol{x})$, its gradient has to be computed. The Jacobian matrix contains derivatives of H with respect to the control vector, and is computed with an adjoint code included in RTTOV. The minimization procedure applies a Marquardt-Levenberg descent algorithm until the convergence criteria are met (see Figure 4). This is the case when the cost function does not change much (about 0.01), the gamma multiplier used in the Marquardt-Levenberg routine is not increasing, and the cost function gradient is sufficiently small (about 1.0). The optimization stops when the solution has converged or a maximum number of iterations (7 iterations in the current implementation) has been exceeded, i.e. the retrieval did not converge. A processing flag is set accordingly and the processing of the next pixel starts.

1D-Var retrievals have the advantage of providing an estimate of the error in the retrieved profile, because 1D-Var retrievals allow the combination of observations with a background estimate in an optimal way, which accounts for the error characteristics of each. The analysis error covariance matrix is an additional output of the NWP SAF 1D-Var for every pixel and impacts the expected retrieval error (see Rodgers, 1990 [RD 4] for more details.
Values for the $\boldsymbol{R}$ matrix were estimated as follows: SSM/I observations were compared with forward simulations of RTTOV using ERA-Interim analysis as input. The resulting standard deviation forms the basis for the uncertainty entries in the $\boldsymbol{R}$ matrix. These uncertainties are interpreted as the sum of observational and model errors. Hence, the uncertainty entries in the R matrix do not only contain uncertainties due to instrument noise but also the uncertainty arising from radiative transfer. The error of the low frequency channels is defined as 2 times the standard deviation while the high frequency channel is defined as 4 times the standard deviation to account for the large sensitivity of this channel to scattering effects.

The $\boldsymbol{R}$ matrix for the 7 channels of SSMI(S) in the non-scattering case is given in Table 2. The letters v and h denote vertical (v) and horizontal (h) polarization. The listed frequencies of the channels are rough values, for the exact values see section 2.1.

Table 2: The $\boldsymbol{R}$ matrix for the 7 channels of SSMI(S) in non-scattering case.

Freq. (GHz)	v19	h19	v22	v37	h37	v85/91	h85/91
Variances (K)	1.8	2.4	1.8	1.8	3.8	12.	20.

Optionally the band-diagonal or the full matrix can be stored as input to the 1D-Var. Here the band-diagonal option is chosen. Therefore the $\boldsymbol{R}$ matrix only contains the band-diagonal values representing the variances of the observation and model errors. These variances are used for all observations being processed. The covariance errors between different channels have not been considered (see section 3.5).

The $\boldsymbol{B}$ matrix used for HOAPS-4.0 is derived from the SSMIS 1D-Var Package of NWP SAF (see http://nwpsaf.eu/site/software/1d-var/previous-packages/1d-var-ssmis-package/). HOAPS-4.0 utilises the NWP SAF MetOffice 1D-Var code but the provided $\boldsymbol{B}$ matrix in this software package does not allow latitudinal variation. Therefore the $\boldsymbol{B}$ matrix file from the SSMIS 1D-Var Package (ATOVS_Bmatrix72_43, see Deblonde, 2002) specifying $\boldsymbol{B}$ matrices for the northern hemisphere, the tropics and the southern hemisphere, serves as basis for the creation of the $\boldsymbol{B}$ matrix used in HOAPS-4.0. The original $\boldsymbol{B}$ matrix was constructed to be latitude dependent more precisely for three geographical zones from south to north, and contains elements separately for ocean and land applications. The $\boldsymbol{B}$ matrix for HOAPS-4.0 is taken from the original B matrix in reverse order (30°N-90°N, 30°N-30°S and 30°S-90°S) and the land elements have not been taken. For every zone the first 43 elements of the $\boldsymbol{B}$ matrix for HOAPS-4.0 contain temperature values in K. The following elements 44-69 contain values for ln(q) in g/kg (bottom 26 levels only). Afterwards elements 70, 71 and 72 contain values for Tsurf, ln(q) at surface and Tskin, respectively. The number of elements of the $\boldsymbol{B}$ matrix corresponds to the number of pressure levels of the variables that are to be retrieved with the 1D-Var. The namelist “Retrieval.NL” provided within the Met Office 1D-Var software package controls the variables that are to be retrieved and provides the mapping between the minimization vector, the radiative transfer model vector and the $\boldsymbol{B}$ matrix (Weston et al., 2013).

3.2 Background profiles

The background or first guess initial states required for the 1D-Var retrieval are estimated from a predefined profile database that has been constructed from the "Diverse profile datasets from the ECMWF 91-level short-range forecasts" by NWP SAF (version 1, Chevallier et al., 2006, [RD 3]).
The dataset contains five collections of profiles simulated by the ECMWF system that have been sampled to represent a wide distribution of atmospheric temperature, water vapour, ozone, cloud condensate and precipitation. Each collection contains 5000 profiles. Roughly 13000 of the profiles are located over ocean and are used to derive the background information.
The profiles have been interpolated to the 43 pressure levels used in the 1D-Var routines. The interpolation is linear in log(pressure).

The background profile that is most consistent with the measured conditions is estimated from the profile data set by NWP SAF (version 1, Chevallier et al., 2006) by constructing a weighted average of several selected profiles, similar to a Bayesian approach as outlined e.g. in Kummerow (1996). The selection is based on sensor derived data and SST only. No further ancillary data, such as water vapour profiles from reanalysis data is used.
In the first step, a subset of profiles is extracted from the profile data base based on the precomputed geophysical parameters: The database is filtered by LWP, water vapour path and SST (SST and water vapour for scattering mode only). Furthermore, a weak latitude filter and a Tb screening is applied to filter out large missmatches.

To determine the individual weights for each profile in the subset, a cost function is calculated similar to equation 3-1:

$$\boldsymbol{J}(\boldsymbol{x}) = \frac{1}{2}\left(\boldsymbol{x} - \boldsymbol{x}^{\boldsymbol{b}}\right)^{\boldsymbol{T}} \boldsymbol{B}^{-1}\left(\boldsymbol{x} - \boldsymbol{x}^{\boldsymbol{b}}\right) + \frac{1}{2}\left[\boldsymbol{H}(\boldsymbol{x}) - \boldsymbol{y}^{\boldsymbol{0}}\right]^{\boldsymbol{T}} \boldsymbol{R}^{-1}\left[\boldsymbol{H}(\boldsymbol{x}) - \boldsymbol{y}^{\boldsymbol{0}}\right] + \frac{1}{2}\mathrm{C} \qquad 3\text{-}2$$

The atmospheric state $\boldsymbol{x}$ is represented by SST, wind speed, TCWV and LWP, while brightness temperatures are all SSMI(S) imager channels plus the polarization differences of the 19, 37 and 85 GHz channels.
The extra penalty (C) is only added to the cost function of profiles, if the retrieval is running in scattering mode. This is not the case for HOAPS-4.0, so that this term is neglegted in the current implementation of the 1D-Var retrieval.

The background profile is then calculated from the weighted average of the selected profiles:

$$\widehat{\boldsymbol{E}}(\boldsymbol{x}) = \sum_{\boldsymbol{j}} \boldsymbol{x}_{\boldsymbol{j}} \frac{\boldsymbol{exp}\left(-\boldsymbol{J}(\boldsymbol{x}_{\boldsymbol{j}})\right)}{\boldsymbol{A}} \qquad 3\text{-}3$$

where A represents the normalization factor:

$$\boldsymbol{A} = \sum_{\boldsymbol{j}} \boldsymbol{exp}\left(-\boldsymbol{J}(\boldsymbol{x}_{\boldsymbol{j}})\right) \qquad 3\text{-}4$$

Theoretically, the background profile can be unphysical in terms of saturation since temperature and humidity are averaged independently. However, individual unphysical temperature or humidity values at a specific layer cannot appear, as none of the averaged profiles contain unphysical values. Moreover, the minimization routine will not allow values that are out of physical limits defined by RTTOV.

3.3 Physical Basis Overview of statistical retrievals

The HOAPS-4.0 parameters near surface specific humidity, latent heat flux, evaporation, precipitation and freshwater flux have been derived with the statistical retrievals as used in HOAPS-3.2. All parameters are derived from SSMI(S) measurements. This section recaps the statistical algorithms and more details on the statistical algorithms can be found in [RD 5].

3.3.1 Near surface specific humidity

A direct measurement of the humidity in the layer directly above the sea surface from satellite soundings is difficult to obtain. Radiometers such as the SSMI(S) measure the radiation that originates from a relatively thick layer rather than from a single level. However, the satellite-retrieved signal contains some information to derive the humidity in the lowest layer of the boundary layer.

The algorithm that is applied here directly relates SSM/I Tbs to the near surface specific humidity q_a. It derives q_a directly from SSMI(S) Tbs using the 19 GHz, 22 GHz, and 37 GHz channels. Bentamy et al. (2003) demonstrated that the chosen combination of SSM/I channels is sufficient for the direct estimation of the near surface specific humidity. The regression model and its coefficients are provided by the following equation:

$$q_a = a_0 + a_1 \cdot Tb_{19V} + a_2 \cdot Tb_{19H} + a_3 \cdot Tb_{22V} + a_4 \cdot T_{37V}$$

where a_0 = -55.9227, a_1 = 0.4035, a_2 = -0.2944, a_3 = 0.3511, and a_4 = -0.2395.

3.3.2 Latent heat flux

The direct measurement of the latent heat flux with space borne sensors is not possible. Here, the parameterization of the latent heat flux Q_l is estimated using the COARE bulk aerodynamic approach of Fairall et al. (1996b, 2003). This method requires the knowledge of near surface wind speed, atmospheric near surface specific humidity, saturation specific humidity and the SST:

$$Q_l = \rho L_E C_E u(q_s - q_a)$$

where ρ is air density, u is the wind speed at 10 meters height (resulting from the 1D-Var), L_E is the specific latent heat of evaporation, C_E is the Dalton number, q_s is the saturation specific humidity at the sea surface, and q_a is the specific humidity at the 10 m. The SST is needed to determine q_s (see section 3.3.3). Turbulent fluxes, like the latent heat flux or the sensible heat flux are derived from bulk formulas using mean values of surface meteorological variables. The COARE bulk flux algorithms are based on the Monin-Obukhov similarity theory (MOST). The basic approach of MOST is to scale the mean and turbulent properties of the dynamical variables by combinations of surface fluxes, while their height dependence is described by the ratio of the height above the surface to the Monin-Obukhov length L (Fairall, 1997, 2003). MOST is one of the most widely used scaling theories in meteorology and has been applied extensively over the ocean and forms the basis of several surface flux estimation methods. Such a model must contain parameterizations for the roughness lengths (or, equivalently, the transfer coefficients) and the empirical profile stability functions Ψ_x. The HOAPS-4.0 latent heat flux is parameterized using the COARE bulk flux algorithm version 2.6a (Bradley et al., 2000), which is an updated version of the COARE 2.5b algorithm (Fairall et al, 1996), based on an extended flux database containing covariance measurements from higher latitudes and under stronger wind conditions. With minor modifications of physics and parameterizations to the version 2.6a, the algorithm is equivalent to the algorithm published as COARE 3.0 by Fairall et al. (2003). The COARE 3.0 algorithm is derived from more than 5000 direct covariance flux measurements collected over the global oceans. Further updates to the previous version 2.5 were a variable Charnock parameter, a new roughness length parameterization for wind speeds up to 20 m/s, and adjustments to the basic profile stability functions to improve the results under near-stable boundary layer conditions. The stability dependent MOST scaling parameters and wind gustiness, which accounts for sub-scale variability, are estimated iteratively in the COARE algorithm. The algorithm is run for each SSMI(S) pixel where all necessary input data are available. Among others, the near surface air temperature is needed. Since it is not possible to measure this parameter directly from space, it is estimated using the mean of two simple bulk approaches:

(a) The satellite derived near surface specific humidity is assumed to be at a constant relative humidity of 80% as proposed by Liu et al. (1994).

(b) A constant temperature difference of 1 K between sea surface and air temperature is assumed (Wells and King-Hele, 1990).

The implementation of the COARE algorithm in HOAPS omits the warm-layer code, since no continuous diurnal cycle information on the surface radiation budget is available from SSMI(S) or AVHRR measurements. These would be needed to infer the warm layer evolution and cool skin effect.

3.3.3 Evaporation

The liquid water evaporation equivalent of the latent heat flux is related to the latent heat flux by:

$$E = Q_l/(L_E \rho_0)$$

where ρ_0 is the freshwater density as a function of temperature (Fairall, 1996).

For the derivation of the evaporation through the bulk formula, the difference in humidity, i.e. sea surface specific humidity minus near surface specific humidity, is calculated. The sea surface saturation specific air humidity is calculated by applying the Magnus formula to the SST input data:

$$e_w = 6.1078 \cdot exp\left[\frac{\mathrm{a}(T - 273.16}{T - \mathrm{b}}\right]$$

where e_w is in [hPa], T is temperature in [K], a= 17.2693882, b=35.86 (Murray, 1967).

An approximate salinity correction to take into account the reduction in vapour pressure caused by a typical salinity of 34 ‰ is applied by scaling the value for pure water with a factor of 0.98 (Sverdrup et al., 1942):

$$e_{w\_sal} = 0.98 \cdot e_w$$

$$q_s = (0.622099 \cdot e_{w\_sal}/(\mathrm{slp} - 0.377901 \cdot e_{w\_sal})$$

where q_s is the saturation specific humidity in [kg/kg]; slp is the sea-level pressure, which is implemented with a constant value of 1013.25 hPa.

The q_s values are calculated individually for each SST observation prior to the gridding and remapping procedures.

3.3.4 Precipitation

A neural network algorithm is used to derive a statistical retrieval for the precipitation from SSMI(S) Tbs. Generally, the ocean surface precipitation algorithm relates an input vector of the measured Tbs to an output vector of the geophysical parameter. The basic principle behind the retrieval is that emission from, and scattering by, cloud and rain particles increases Tbs at low frequencies and decreases Tbs at high frequencies relative to the radiometrically cold sea surface. Therefore microwave based retrievals of precipitation are based on the direct interaction of the radiation field and the hydrometeors (water droplets, ice particles). The neural network was trained with precipitation rates retrieved from assimilated Tbs in a 1D-Var scheme from the ECMWF. The training data set for the neural network is based on radiative transfer calculations as described in Bauer et al. (2006a,b). The data set contains one month (August 2004) of assimilated SSM/I Tbs and the corresponding ECMWF 1D-Var retrieved precipitation values of the ECMWF model. Using precipitation values from the operational variational analysis to compile the training data set not only ensures the statistical representativeness of the input data, it also makes use of the advantage to have the background meteorological surface fields and profiles consistent with the measured SSM/I brightness temperatures. Moreover, it allows to construct a training data set from a large number of samples based on a sophisticated radiative transfer model. This data set contains a wide variety of globally distributed rainfall events including extreme rainfall in hurricanes and snowfall at high latitudes. For more details on the neural network architecture of the precipitation retrieval algorithm see [RD 5] and Andersson et al. (2010). The resulting HOAPS precipitation retrieval is a statistical algorithm which only depends on SSMI(S) Tbs as input and does not need a first guess or other ancillary data.

3.3.5 Freshwater flux

The freshwater flux at the sea surface is defined as positive for a flux that is directed from the ocean into the atmosphere. If precipitation and evaporation are retrieved the freshwater flux is computed as the difference of evaporation minus precipitation. The freshwater flux product is not computed directly from the SSMI(S) swath data, since the concurrent retrieval of precipitation and evaporation is generally not possible in presence of precipitation.
In order to retrieve the freshwater flux, the input parameters precipitation and evaporation are averaged separately onto the HOAPS grid on a monthly basis. Then the freshwater flux is computed for the gridded data products for each grid box as the difference between the spatial and temporal means of evaporation and precipitation. In certain regions with frequent precipitation this method may introduce a clear sky bias from the evaporation fields in the resulting freshwater flux fields.

3.4 Uncertainty estimates and post-processing

The gridding routines enabling the processing from swath based HOAPS L2 data to gridded and averaged HOAPS L3 data remain unchanged relative to HOAPS-3.2 and are described in RD 9. Furthermore the turbulent flux parameters are calculated in the post-processing.
Additionally systematic and random retrieval uncertainties to all L2 evaporation-related geophysical parameters are assigned. A comprehensive DWD-ICOADS data archive serves as the in situ ground reference. As the in situ ground reference buoy and ship observations were used: The buoy and ship observations were collected and quality controlled with a High Quality Control (HQC) procedure at the Marine Data Centre of DWD (located in the Hamburg Marine Meteorological Office of DWD, Seewetteramt, http://www.dwd.de/EN/ourservices/marine_data_centre/maritimesdatenzentrum.html).
Missing data in the DWD data set were filled with ICOADS (International Comprehensive

Ocean-Atmosphere Data Set) data before the quality control routines were applied, see also Kinzel et al. (2016).
The assignment of the systematic uncertainties is carried out by applying multi-dimensional bias look-up tables as a function of the concurrent atmospheric state; here based on wind speed, near-surface specific humidity, SST and integrated water vapour. Using the DWD-ICOADS data as reference, a four-dimensional bias look-up table is spanned, with equally distributed number of bin entries. A more detailed description of the construction of the four-dimensional bias look-up table, where the dimensions correspond to wind speed, near surface specific humidity, SST and integrated water vapour is given in Kinzel et al. (2016). On basis of the look-up table the systematic uncertainty is defined while the random uncertainty is the associated spread. Respective uncertainties of the latent heat flux and evaporation are derived via standard error propagation. This includes uncertainty estimates of the transfer coefficient, which are estimated after Fairall et al. (2003) and Gleckler and Weare (1997). Likewise, random uncertainties are derived. The following systematic uncertainty estimates for the transfer coefficient have been used: 5 % for wind speeds ≤ 10 m/s, 10 % for wind speeds ≥ 10 m/s, and 12 % for wind speeds ≥ 20 m/s. 20 % are assumed as random uncertainty estimates of the transfer coefficient.
To isolate the retrieval contribution from the overall random uncertainty, random uncertainties decomposition via multiple triple collocation was carried out, following the approach of Kinzel et al. (2016).
Selected geophysical parameters are additionally equipped in L3 with externally derived sampling uncertainties, following the approach of Tomita and Kubota (2011).

3.5 Assumptions and Limitations

The retrieval is only applicable over the ice-free open sea. Surface parameters like wind and near surface humidity (and consequently turbulent fluxes) cannot be retrieved for scenes affected by heavy precipitation. If the a-priori information exhibits significant mismatches with the underlying “real” weather scene, the 1D-Var may not converge. If no a-priori profile could be constructed for the underlying weather scene the 1D-Var is not run for that scene.
The current implementation of the 1D-Var does not utilise covariances of errors between different channels. It is anticipated that the estimation of the covariances of errors is very complicated as it will depend not only on Tbs but also on atmospheric conditions and instrument characteristics, here in particular the heating and cooling depending on position relative to Sun/Earth. Thus the $\boldsymbol{R}$ matrix would ideally be recomputed for every pixel and time. In consequence, associated processing would be computationally very expensive. The covariance of errors between different channels is assumed to be relatively small because the spectral separation is relatively large, with the exception of the vertically and horizontally polarised channels. Deblonde (2002) assumes that the instrument and forward model errors are not correlated between channels.
Assumptions and limitations for the geophysical parameters near surface specific humidity, precipitation, latent heat flux, evaporation and freshwater flux given in RD 5 are still valid. A summary is given in the following.
As the implemented retrievals are statistical procedures, the retrievals are only as good as the quality of the input data set and how they represent the atmospheric state. The training data for the retrievals for near surface specific humidity, latent heat flux and thus evaporation originates from ship data. Therefore not all regions and hence atmospheric situations may be equally well represented in the training data set. Another general issue in the training data set is that the buoy data consists of temporal averages of point measurements which are related to area averages of the SSM/I footprint. This introduces additional scatter into the data through the different scales of the data. However, the number of samples in the input data is large enough, to compensate for this. For the precipitation retrieval the well established ECMWF radiative transfer and assimilation schemes are used to generate the

input data. The quality of the statistical precipitation retrieval therefore depends on the physical ECMWF 1D-Var retrieval.
The retrieval for the near surface specific humidity is not possible for atmospheric situations with high liquid water content or high rain water content, because the strong emission from atmospheric water masks the signal. High water content values above 80 g/kg within the sampled pixels are therefore treated as undefined. In scenes over very warm water masses with high air humidity the satellite-retrieved q_a signal tends to saturate. This leads to a tendency to underestimate q_a for values above 20 g/kg.
The COARE algorithm applied to derive the latent heat flux and subsequentially the evaporation depends on a few assumptions, but the main limitations stem from the satellite retrieved input parameters wind speed, near surface specific humidity, and sea surface saturation specific humidity (derived from SST). Among others, the near surface air temperature is needed as input. Since it is not possible to measure this parameter directly from space, it is estimated using the mean of two simple bulk approaches (see section 3.3.2). On climatological scale these assumptions are valid for the majority of oceanic conditions. However, in regions with strong stable stratification of the atmospheric surface layer, this approach will affect the quality of sensible heat flux estimates. The impact of these assumptions on the latent heat flux retrieval is smaller since the air temperature is not directly used in the bulk formula and has only a secondary effect on the parameterization as it is used in the stability estimation of the atmosphere (Liu et al., 1994).

Due to the inability to derive the surface wind speed from SSMI(S) in cases of high atmospheric water content, i.e. precipitation, no values are retrieved for such situations. Hence, it is only possible to retrieve evaporation in situation with no or light rain. The use of daily mean SST fields may lead to errors in the flux estimates in certain regions with a strong diurnal cycle of the SST. The COARE algorithms include a module to estimate the diurnal evolution of the oceanic warm layer. This part is disabled in the HOAPS retrieval, as it would require continuous radiative flux measurements for the whole day, which are not available from SSMI(S). The COARE 2.6a/3.0 parameterizations are derived from flux measurements data containing situations with wind speeds in the range of 0-20 m/s. The accuracy described by Fairall (2003) is within 5% for wind speeds of 0–10 m/s and 10% for wind speeds between 10 and 20 m/s. For higher wind speeds the accuracy may decrease further. Although the underlying data base has been extended for the recent versions of the COARE algorithm, most of the data stems from tropical regions of the pacific. However, there seem to be no implications for global application of the algorithm from this limitation as Brunke et. al. (2003) found the COARE algorithm to be one of the least problematic in a comparison of different bulk flux estimates over the tropical and midlatitude oceanic regions.

A general limitation of the precipitation retrieval is the detectability of precipitation at low rain rates. The current retrieval uses a lower cutoff value of 0.3 mm/h. Hence, these light rain events are not captured by the retrieval.

The freshwater flux product relies on the output of the individual HOAPS algorithms for evaporation and precipitation. Since it is not possible to retrieve the evaporation in situation with precipitation (except for light rain), the freshwater flux cannot be determined for individual SSMI(S) pixels in these cases. Instead it is computed for each grid box as the difference of the spatially and temporally averaged evaporation and precipitation fields. These averages may contain different numbers of observations. Thus no statistical variables like the number of observations or standard deviation are available in the gridded freshwater flux data products. The largest effect on the mean freshwater flux fields by this clear sky bias is observed over the Southern Ocean, the ITCZ, where in 10% to 15% of all SSMI(S) observations the retrieval of wind speed, near surface humidity, and hence evaporation is not possible. The systematic omission of potentially extreme deviations from the mean values or from the surrounding area may result in biases. However, even under the extreme assumption of 100% error for the missed evaporation estimates, this would not result in more than about 10-15% error for the monthly mean in the most affected regions (see also [RD 8]). Evaporation and precipitation often have of the same order of magnitude. Thus the resulting values in the freshwater flux fields are sensitive to relatively small variations in either of the input parameters. Small errors in one of the input parameters may lead to larger deviations in the resulting freshwater flux fields. This effect decreases with longer temporal and/or larger spatial averages.

4 References

Andersson, A., Fennig, K., Klepp, C., Bakan, S., Graßl, H., and Schulz, J., 2010: The Hamburg Ocean Atmosphere Parameters and Fluxes from Satellite Data – HOAPS-3, *Earth Syst. Sci*. Data, **2**, 215-234, doi:10.5194/essd-2-215-2010.

Bauer, P., Lopez, P., Benedetti, A., Salmond, D., and Moreau, E., 2006a: Implementation of 1D+4D-Var Assimilation of Precipitation-affected Microwave Radiances at ECMWF, 2006a: I: 1D-Var, Q. J. Roy. Meteor. Soc., **132**, 2277-2306.

Bauer P, E. Moreau, F. Chevallier, and U. O'Keeffe, 2006b: Multiple-scattering microwave radiative transfer for data assimilation applications. Q. J. R. Meteorol. Soc. **132**, 1259–1281.

Bentamy, A., Katsaros, K. B., Mestas-Nunez, A. M., Drennan, W. M., Forde, E. B., and Roquet, H., 2003: Satellite Estimates of Wind Speed and Latent Heat Flux Over the Global Oceans, J. Climate, **16**, 637-656.

Bradley, E. F., Fairall, C. W., Hare, J. E., and Grachev, A. A., 2000: An Old and Improved Bulk Algorithm for Air-sea Fluxes: COARE 2.6 A, in: Preprints, 14th Symp. on Boundary Layers and Turbulence, Aspen, CO, Am. Meteorol. Soc., 294–296.

Brunke, M. A., C. W. Fairall, X. Zeng, L. Eymard, and J.A. Curry, 2003: Which bulk aerodynamic algorithms are least problematic in computing ocean surface turbulent fluxes? J. Climate, **16**, 619-635.

Chevallier, F., S. Di Michele and A. P. McNally, 2006: Diverse profile datasets from the ECMWF 91-level short-range forecasts, Version 1.0, Document No.: NWPSAF-EC-TR-010.

Deblonde, G., 2001: Stand-alone 1D-Var scheme for the SSM/I, SSMIS and AMSU. User's Guide version 1.0., NWP SAF

Deblonde, G., 2002: Stand-alone 1D-Var scheme for the SSM/I, SSMIS and AMSU. User's Guide version 2.0., NWP SAF

Deblonde, G., Mahfouf, J.F. and Bilodeau, B., 2007: One-dimensional variational data assimilation of SSM/I observations in rainy atmospheres at MSC. *Mon Weather Rev*, **135**(1): 152-172.

Donlon, C. J., P. J. Minnett, C. Gentemann, T. J. Nightingale, I. J. Barton, B. Ward, and M. J. Murray, 2002: Toward Improved Validation of Satellite Sea Surface Skin Temperature Measurements for Climate Research. J. Climate, **15**, 353-369, doi: 10.1175/1520-0442(2002)015<0353:TIVOSS>2.0.CO;2.

Eyre, J.R., 1989: Inversion of Cloudy Satellite Sounding Radiances by Nonlinear Optimal Estimation .1. Theory and Simulation for TOVS. *Q J Roy Meteor Soc*, **115**(489): 1001-1026.

Fairall, C. W., E. F. Bradley, D. P. Rogers, J. B. Edson, and G. S. Young, 1996: Bulk Parameterization of Air-sea Fluxes for Tropical Ocean-Global Atmosphere Coupled Ocean-Atmosphere Response Experiment. J. Geophys. Res., **101**, 3747-3764.

Fairall, C. W., E. F. Bradley, J. E. Hare, A. A. Grachev, and J. B. Edson, 2003: Bulk Parameterization of Air-Sea Fluxes: Updates and Verification for the COARE algorithm. J. Climate, **16**, 571-591.Fennig, K.; Andersson, A.; Schröder, M., 2015: Fundamental Climate Data Record of SSM/I / SSMIS Brightness Temperatures. Satellite Application Facility on Climate Monitoring. DOI:10.5676/EUM_SAF_CM/FCDR_MWI/V002. http://dx.doi.org/10.5676/EUM_SAF_CM/FCDR_MWI/V002.

Ferraro, R. R., 1997: SSM/I derived global rainfall estimates for climatological applications, *J. Geophys. Res.*, **102**, 16715-16735.

Gleckler, P. J. and B. C. Weare, 1997: Uncertainties in Global Ocean Surface Heat Flux Climatologies Derived from Ship Observations, J. Climate, **10**, 2764-2781.

Gruss, M., 2016: U.S. Air Force blames power failure for loss of DMSP-F19 weather satellite, SpaceNews article from July 25, 2016, accessible at http://spacenews.com/u-s-air-force-blames-power-failure-for-loss-of-dmsp-f19-weather-satellite/.

Hocking, J., P.Rayer, D. Rundle, R. Saunders, M. Matricardi, A. Geer, P. Brunel and J. Vidot, 2014: RTTOV v11 Users Guide, version 1.3, available at https://nwpsaf.eu/deliverables/rtm/docs_rttov11/users_guide_11_v1.3.pdf.

Kinzel, J., K. Fennig, M. Schröder, A. Andersson, K. Bumke, and R. Hollmann, 2016: Decomposition of Random Errors Inherent to HOAPS-3.2 Near-Surface Humidity Estimates Using Multiple Triple Collocation Analysis, *J. Atm. Oceanic Tech.*, 1455-1471, 33 (7), doi:/10.1175/JTECH-D-15-0122.1.

Kummerow, C.; Olson, William S.; Giglio, L., 1996: A simplified scheme for obtaining precipitation and vertical hydrometeor profiles from passive microwave sensors, *Geoscience and Remote Sensing*, IEEE Transactions on , **34**, no.5, pp.1213-1232, doi: 10.1109/36.536538.

Kunkee, D.B., Poe, G.A., Swadley, S.D., Hong Y., Wessel J.E., and Uliana E.A., 2008: Desgin and Evaluation of the First Special Sensor Microwave Imager/Sounder, IEEE Trans. *Geosci. Remote Sens*., **46**, 863-883.

Liu, W., Zhang, A., and Bishop, J.: Evaporation and solar irradiance as regulators of sea surface temperature in annual and interannual changes, J. Geophys. Res., 99, 12623–12638, 1994.

Minnett P., A. Kaiser-Weiss, 2012: Discussion document: Near-surface oceanic temperature gradients. Available from https://www.ghrsst.org/science-and-applications/sst-definitions/.

Murray, F. W., On the computation of saturation vapor pressure, *J. Appl. Meteorol.*, **6**, 203-204, 1967.

Olson, W. S., C. D. Kummerow, Y. Hong, and W-K. Tao. 1999: Atmospheric latent heating distributions in the Tropics derived from satellite passive microwave radiometer measurements. *J. Appl. Meteor* **38**:633–664.

Phalippou, L., 1996: Variational retrieval of humidity profile, wind speed and cloud liquid-water path with the SSM/I: Potential for numerical weather prediction. *Q J Roy Meteor Soc*, **122**(530): 327-355.

Reynolds, R. W., N. A. Rayner, T. M. Smith, D. C. Stokes, and W. Wang, 2002: An improved in situ and satellite SST analysis for climate. *J. Climate*, **15**, 1609–1625.

Reynolds, R. W., T. M. Smith, C. Liu, D. B. Chelton, K. S. Casey, and M. G. Schlax, 2007: Daily High-Resolution-Blended Analyses for Sea Surface Temperature. *J. Climate*, **20**, 5473–5496, doi: http://dx.doi.org/10.1175/2007JCLI1824.1.

Reynolds, R. W., 2009: What's New in Version 2. OISST Webpage. http://www.ncdc.noaa.gov/sites/default/files/attachments/Reynolds2009_oisst_daily_v02r00_version2-features.pdf.

Rodgers, C.D., 1976: Retrieval of Atmospheric-Temperature and Composition from Remote Measurements of Thermal-Radiation. *Rev Geophys*, **14**(4): 609-624.

Rodgers, C.D., 1990: Characterization and error analysis of profiles retrieved from remote sounding measurements. *J. Geophys. Res*., **95**, 5587-5595.

Rodgers, C.D., 2000: Inverse methods for atmospheric sounding: Theory and practice, 2. World scientific Singapore.

Sverdrup, H. U., M. W. Johnson, R. H. Fleming: The Oceans, Their Physics, Chemistry, and General Biology. New York: Prentice-Hall, c1942 1942. http://ark.cdlib.org/ark:/13030/kt167nb66r/.

Tomita, H. and M. Kubota, 2011: Sampling error of daily mean surface wind speed and air specific humidity due to Sun-synchronous satellite sampling and its reduction by multisatellite sampling, International *Journal of Remote Sensing*, **32**, 3389-3404, doi: 10.1080/01431161003749428.

Wells, N. and King-Hele, S.: Parametrization of tropical ocean heat flux, Q. J. Roy. Meteor. Soc., 116, 1213–1224, 1990.

Weston, P., E. Pavelin, A. Collard, 2013: NWPSAF UK Met Office 1D-Var User Manual, version 3.5, available at https://nwpsaf.eu/deliverables/metoffice_1dvar/nwpsaf-mo-ud-006_NWPSAF_1DVar_Manual.html

Woodruff, S. D., and Coauthors, 2011: ICOADS release 2.5: Extensions and enhancements to the surface marine meteorological archive. *Int. J. Climatol.*, **31**, 951–967.